Available online at www.sciencedirect.com
ScienceDirect
Journal of the European Ceramic Society 31 (2011) 1191–1198
www.elsevier.com/locate/jeurceramsoc

Microstructure, growth mechanism and mechanical property of Al_2O_3-based eutectic ceramic *in situ* composites

Jun Zhang *, Haijun Su, Kan Song, Lin Liu, Hengzhi Fu

State Key Laboratory of Solidification Processing, Northwestern Polytechnical University, Xi'an 710072, PR China

Available online 8 December 2010

Abstract

Directionally solidified Al_2O_3-based eutectic ceramic *in situ* composites with inherently high melting point, low density, excellent microstructure stability, outstanding resistance to creep, corrosion and oxidation at elevated temperature, have attracted significant interest as promising candidate for high-temperature application. This paper reviews the recent research progress on Al_2O_3-based eutectic ceramic *in situ* composites in State Key Laboratory of Solidification Processing. Al_2O_3/YAG binary eutectic and Al_2O_3/YAG/ZrO_2 ternary eutectic ceramics are prepared by laser zone melting, electron beam floating zone melting and laser direct forming, respectively. The processing control, solidification characteristic, microstructure evolution, eutectic growth mechanism, phase interface structure, mechanical property and toughening mechanism are investigated. The high thermal gradient and cooling rate during solidification lead to the refined microstructure with minimum eutectic spacing of 100 nm. Besides the typical faceted/faceted eutectic growth manner, the faceted to non-faceted growth transition is found. The room-temperature hardness H_V and fracture toughness K_{IC} are measured with micro-indentation method. For Al_2O_3/YAG/ZrO_2, $K_{IC} = 8.0 \pm 2.0$ MPa m$^{1/2}$ while for Al_2O_3/YAG, $K_{IC} = 3.6 \pm 0.4$ MPa m$^{1/2}$. It is expectable that directionally solidified Al_2O_3-based eutectic ceramics are approaching practical application with the advancement of processing theory, technique and apparatus.

Keywords: Al_2O_3-based ceramic; Eutectic *in situ* composite; Microstructure; Growth mechanism; Mechanical property

1. Introduction

In recent years, due to the unique properties, directionally solidified (DS) oxide eutectic *in situ* composites have been considered as new generation of structural or functional materials with high performance especially serviced at high temperatures.[1–4] The alumina-based eutectic *in situ* composites with high melting point of about 2100 K, low density (<5 g/cm^3), excellent specific strength, superior oxidation and creep resistance, and outstanding microstructure stability at elevated temperatures up to 2073 K, have attracted significant interest as one of the most promising candidates for ultra-high temperature structural materials applied to the high temperature oxidizing atmosphere over a long period of time.[5–8] Furthermore, it is also very important to reveal the faceted eutectic growth manner of Al_2O_3-based ceramic for development of eutectic solidification theory, which is extraordinarily imperfect yet in many respects for irregular faceted eutectic growth mechanism. Up to now the solidification characteristics of Al_2O_3-based ceramic have not been well understood.[4,9]

Several directional solidification techniques have been developed to prepare oxide eutectic composites, such as Bridgman method,[5,6] laser floating zone (LFZ) method,[7,8] edge-defined film-fed growth (EFG) method[10] and micro-pulling down (μ-PD) method.[11] Since most Al_2O_3-based eutectics have extremely high melting points, it is very difficult to prepare them with the conventional directional solidification methods and equipments, which leads to the urgent requirement to develop new preparation technique. With advantages of very high melting temperature, absence of possible crucible or die contamination, steep thermal gradient of above 10^4 K/cm at solidification interface, and rapid solidification rate, the laser zone melting technique has been successfully used to grow oxide eutectic composites.[12–14]

This paper reviews the recent research progress on Al_2O_3-based eutectic ceramic *in situ* composites in State Key Laboratory of Solidification Processing. The directionally solidified Al_2O_3/YAG binary eutectic and Al_2O_3/YAG/ZrO_2 ternary eutectic *in situ* composites are prepared by the laser zone melting technique (LZM), the modified electron beam float-

* Corresponding author. Tel.: +86 29 88494825; fax: +86 29 88494825.
E-mail addresses: zhjscott@nwpu.edu.cn, shjnpu@nwpu.edu.cn (J. Zhang).

0955-2219/$ – see front matter © 2010 Elsevier Ltd. All rights reserved.
doi:10.1016/j.jeurceramsoc.2010.11.008

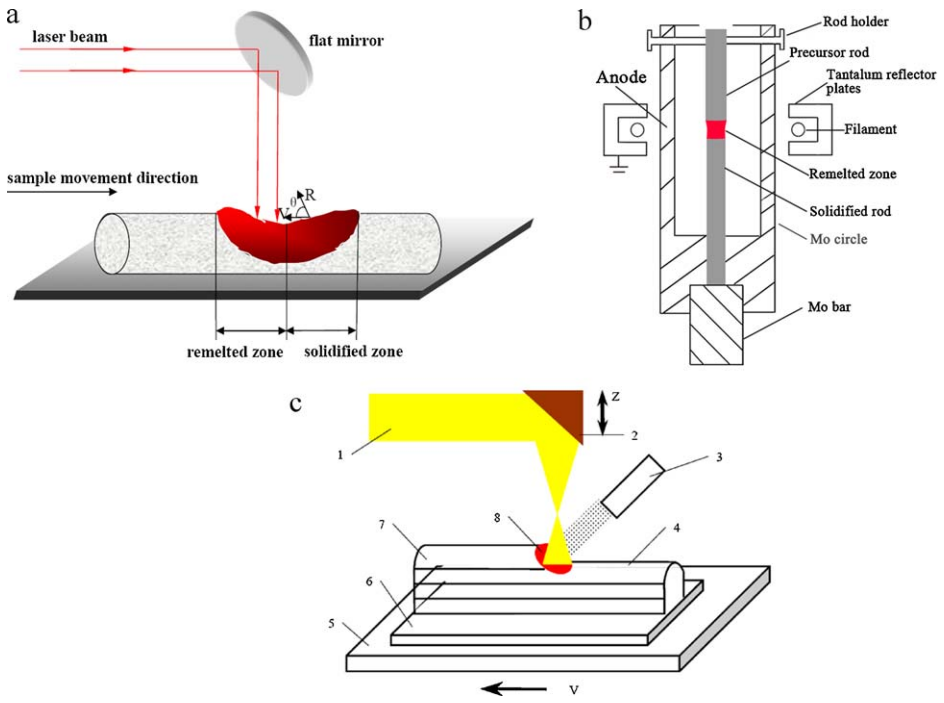

Fig. 1. Solidification preparation procedure of oxide eutectic: (a) laser zone melting (V is the scanning rate, R is the solidification rate, and θ is the solidification direction angle); (b) modified electron beam floating zone melting; (c) laser direct forming (1, laser; 2, mirror; 3, JPSF-1 powder feeder; 4 and 7, solidified layer; 5, worktable; 6, substrate; 8, melting zone).

ing zone melting technique (MEBFZM) and the laser direct forming technique (LDF). The relationships between the solidification parameter, the solidification microstructure and the mechanical property of Al_2O_3-based eutectic composites are systematically studied. Moreover, the phase interface structure, the microstructure characteristic and evolution, and the eutectic growth mechanism are investigated.

2. Experimental

2.1. Precursor

Al_2O_3, Y_2O_3 and ZrO_2 nano-powders with high purity (>4 N) are homogenously mixed by wet ball milling according to binary eutectic composition[15] of Al_2O_3:Y_2O_3 = 82:18 and ternary eutectic composition[16] of Al_2O_3:Y_2O_3:ZrO_2 = 65.8:15.6:18.6 (mol%), respectively. Ø7 mm × 60 mm rod precursor and 68 mm × 7 mm × 5 mm plate precursor are prepared by die pressing at 25 MPa for 10 min and are then sintered at 1773 K for 2 h to obtain the precursor density of about 2–3 g/cm^3.

2.2. Laser zone melting (LZM)

The laser zone melting is carried out in a vacuum chamber with 5 kW ROFIN-SINAR850 CO_2 laser. The precursor sample is moved by the numerically controlled worktable with 5-axis and 4-direction coupled motion to realize the laser beam scanning along the sample axis, as illustrated in Fig. 1a. The precursor is first rapidly remelted to form the melting zone and then solidified just behind the melting zone to obtain the directionally solidified sample with smooth surface and high density. During the melting, two beams of high-purity Ar gas are inputted into the vacuum chamber from the top and bottom of the substrate at the flow speed of 10 L/min. The laser power is 190–220 W and the scanning rate is 10–2000 μm/s. The deepness of the solidified layer is 0.5–3 mm for the plate. The diameter of the solidified rods is about 4–6 mm. The detailed process has been described elsewhere.[14]

2.3. Modified electron beam floating zone melting (MEBFZM)

The experiment is performed in the ESZ1.5/5 electron beam floating zone melting furnace. As the precursor is nonconductive, a special Mo anode is served as heating element to realize the floating zone melting. The MEBFZM sketch is shown in Fig. 1b. With the electron gun, consisting of the cathode filament and the focusing system, moving upward, the precursor is first zone-melted and then directionally solidified. The solidified eutectic sample can be prepared by accurate control of the solidification processing as described elsewhere.[17]

2.4. Laser direct forming (LDF)

As the precursors are all required for the two methods above, the processing is complex and time consuming. In order to simplify the preparation processing, the laser direct forming technique is used as shown in Fig. 1c, which is a promising technique to manufacture three-dimensional component. The mixed oxide powders with eutectic composition are sprayed out from the feeder nozzle and are rapidly melted by the scanning laser beam to create a moving molten pool. The eutectic composite

Table 1
Representative processing parameters in the laser direct forming.

Laser power (W)	Scanning rate (mm/min)	Beam diameter (mm)	Powder feed rate (g/s)	Shielding Ar gas flow rate (L/min)
190–220	5–15	4	0.1–0.2	10

is formed layer by layer with the solidification of molten pool. The processing parameters are listed in Table 1.

2.5. Characterization

The microstructure and the phase are characterized with scanning electron microscopy (SEM, JSM-5800), transmission electron microscopy (TEM, JEM-200CX), energy disperse spectroscopy (EDS, Link-Isis), X-ray diffraction (XRD, Rigakumsg-158), and digital image analysis (SISC IAS V8.0) for quantitative calculation. The room-temperature hardness H_V and fracture toughness K_{IC} of laser remelted Al_2O_3/YAG and Al_2O_3/YAG/ZrO_2 eutectics are determined by Vickers microindentation technique with load of 9.8 N for 15 s.

3. Results and discussion

3.1. Solidification microstructure

Fig. 2 shows the typical microstructure of laser remelted Al_2O_3/YAG and Al_2O_3/YAG/ZrO_2 eutectics grown under the same solidification condition. Al_2O_3/YAG eutectic consists of α-Al_2O_3 (the black) and YAG (the gray) phases without any other phases. The phase volume ratio is Al_2O_3:YAG = 46:54, which coincides well with that expected for eutectic composition. The eutectic presents an interpenetrating network as "Chinese Script" type structure, in which Al_2O_3 and YAG phases are homogenously distributed and interconnected with each other without grain boundary. Compared with binary eutectic, Al_2O_3/YAG/ZrO_2 eutectic has three phases of α-Al_2O_3 phase (the black), YAG phase (the gray) and c-ZrO_2 phase (the white). The phase volume ratio is Al_2O_3:YAG:ZrO_2 = 40:43:17. YAG and Al_2O_3 with similar size are continuously interwoven with each other, while ZrO_2 is mainly distributed at the Al_2O_3/YAG interface. The eutectic spacing of Al_2O_3/YAG/ZrO_2 is much smaller than that of Al_2O_3/YAG, which indicates that the addition of ZrO_2 can effectively refine the eutectic microstructure.

With fixed laser power, the laser scanning rate dominates the microstructure characteristic and evolution. As the thermal gradient of solidification interface during LZM can be as high as 10^4–10^5 K/cm, the coupled eutectic growth can be maintained even at high scanning rate. It is shown in Fig. 3 that the phase size and interspacing are all greatly reduced but the phase shape is not changed when the scanning rate is increased, which is well consistent with the results of Lee et al.[18] and Peña et al.[19] The microstructure refinement is mainly ascribed to the rapid solidification as well as the addition of the third component ZrO_2.

Fig. 4 shows the microstructure of Al_2O_3/YAG eutectic prepared by MEBFZM technique at different growth rates. The microstructure morphology is quite similar to that of laser remelted Al_2O_3/YAG eutectic but the eutectic spacing is augmented due to the relatively low thermal gradient (about 300–500 K/cm) of solidification interface.[20] Meanwhile, the eutectic phases tend to grow along the solidification direction due to the intensively directional thermal flow. The relationship between the eutectic spacing (λ) and the growth rate (v) is $\lambda = 6.7v^{-1/2}$, where λ is in μm and v in μm/s.

Fig. 5 shows the microstructure of Al_2O_3/YAG eutectic grown by LDF. The eutectic spacing can be fine as 100 nm due to the very high thermal gradient leading to rapid cooling rate, while Calderon-Moreno and Yoshimura[21] has obtained Al_2O_3/ZrO_2 eutectic with interspacing of 30 nm by melt quenching technique. In order to obtain large sample, further investigation is still undergoing especially to enhance the stability and matching of the technical parameters such as powder type, powder feeding manner, shielding gas flow rate, etc.

Since the solidification microstructure is very complex and irregular, it is quite difficult to quantificationally depict it by conventional method. However, as shown in Fig. 6, the oxide eutectic microstructure can be quantitatively characterized by

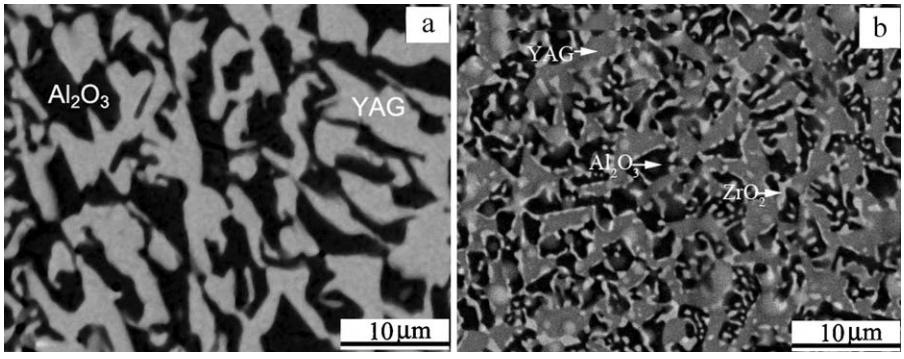

Fig. 2. Typical solidification microstructures of the laser remelted (a) Al_2O_3/YAG binary eutectic and (b) Al_2O_3/YAG/ZrO_2 ternary eutectic grown at the scanning rate of 20 μm/s.

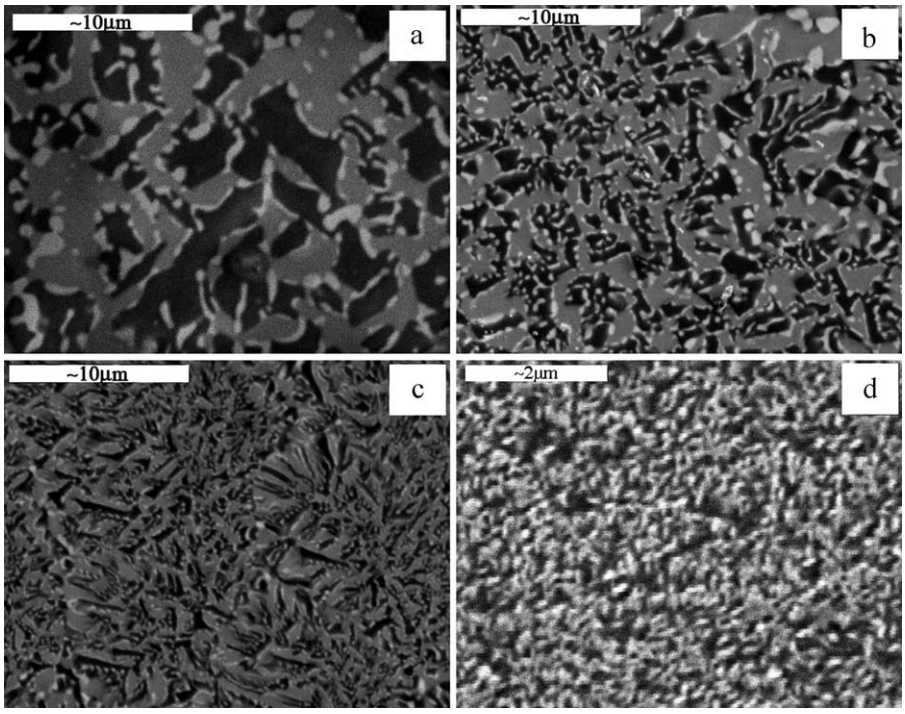

Fig. 3. Microstructures of the transverse sections of the laser remelted Al_2O_3/YAG/ZrO_2 ternary eutectics grown at different scanning rates: (a) 20 μm/s; (b) 100 μm/s; (c) 200 μm/s; (d) 1000 μm/s.

the fractal analysis, which has now become an effective way to analyze the complex microstructures of metals, alloys and ceramics.[22,23] The fractal dimension of the eutectic microstructure increases with the increased scanning rate (Fig. 6a), which suggests that the complexity of the microstructure increases at high scanning rate. Meanwhile with the decrease of the eutectic spacing, the fractal dimension increases (Fig. 6b). However, it is found that the fractal characteristic is not obvious at further high scanning rate due to the appearance of cellular microstructure.

3.2. Interface structure and eutectic growth mechanism

The phase interface characteristic plays an important role on microstructure and property of composite material. Since there are huge amounts of intrinsic and clean interfaces between eutectic phases in directionally solidified oxide eutectics, the eutectic *in situ* composite can retain superior property even at temperature near to its melting point. Fig. 7 presents the phase interface in directionally solidified Al_2O_3/YAG eutectic. The

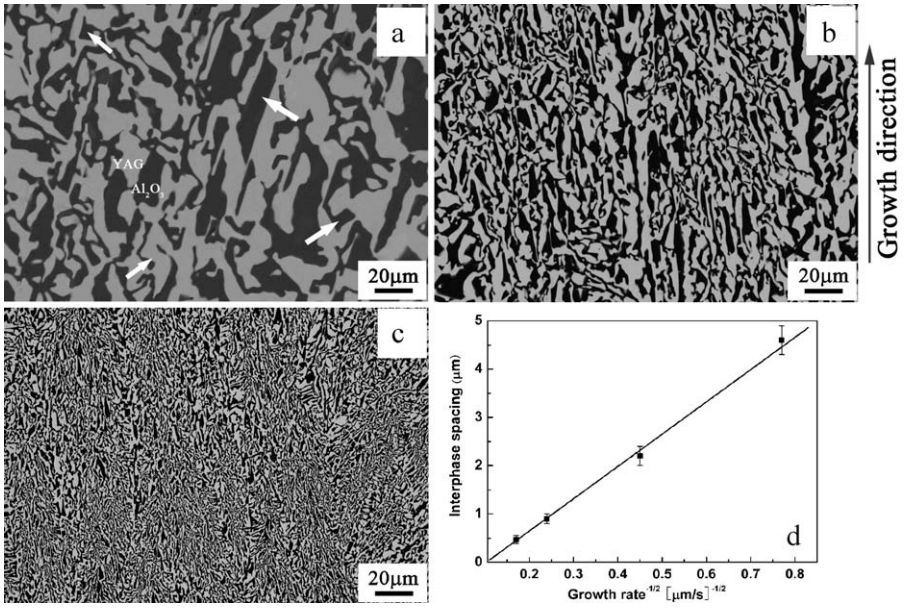

Fig. 4. Typical microstructures of the longitudinal sections of the DS Al_2O_3/YAG eutectics grown by the MEBFZM technique at different rates: (a) 1.7 μm/s; (b) 5 μm/s; (c) 16.7 μm/s; (d) the relationship between the mean interphase spacing and growth rate[17].

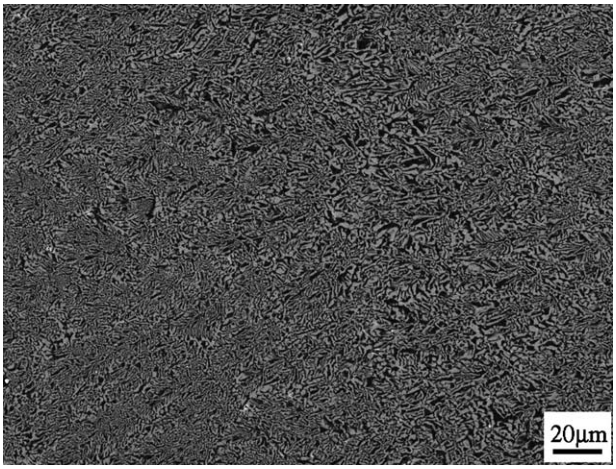

Fig. 5. Typical microstructure of the Al_2O_3/YAG eutectic grown by the LDF technique at the scanning rate of 167 μm/s.

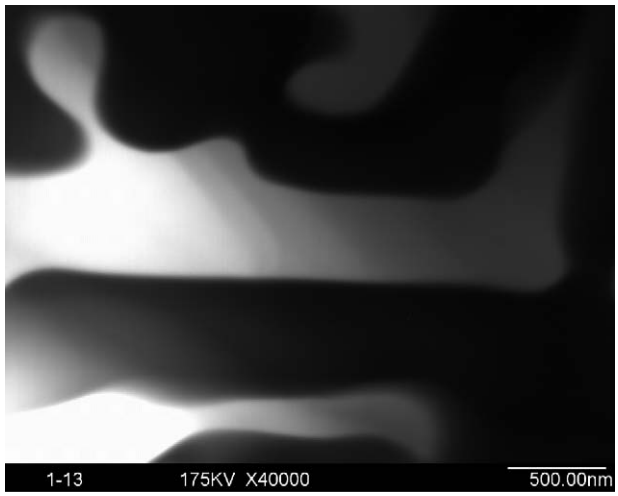

Fig. 7. TEM morphology of the interface of the eutectic phases in the Al_2O_3/YAG binary eutectic.

interfaces are smooth and clear without any other phase, which indicates that the eutectic phases with low-energy interface can bond with each other very well.

As is well known, the directionally solidified eutectic usually presents preferential growth along well-defined crystallographic directions. However, the oxide eutectic with very strong anisotropic growth characteristic tends to display an interconnected microstructure, so the oxide eutectic may present two sets of orientation relations.[4] In terms of Jackson–Hunt (J-H) theory,[24] the eutectic can be categorized according to the growth characteristic of eutectic phases as non-faceted/non-faceted eutectic, faceted/non-faceted eutectic and faceted/faceted eutectic, which may exhibit regular or irregular morphology. When the fusion entropy ΔS is high and $\Delta S/R > 2$, where R is gas constant, the phase presents faceted growth manner. And if $\Delta S/R > 5$, the phase possesses strongly faceted growth behavior. Thus if one of the eutectic phases is faceted, the irregular or complex microstructure is formed. Since $\Delta S_{Al_2O_3}$ is 48 J/(K mol), ΔS_{YAG} is 122 J/(K mol), and ΔS_{ZrO_2} is 30 J/(K mol), Al_2O_3 and YAG have high value of $\Delta S/R > 5$ and the value $\Delta S/R$ of ZrO_2 is just slightly larger than 2. Therefore, Al_2O_3 and YAG show typically faceted growth manner to form polyhedral shapes, whereas ZrO_2 tends to grow with weakly faceted or non-faceted manner to form rod or slice shapes. As the rapid growth of Al_2O_3 and YAG with large volume fraction dominates the eutectic solidification, the coupled growth of eutectic phases cannot be kept and the eutectic spacing is no longer constant, which consequently leads to the irregular growth morphology. It can be concluded that the faceted growth is the most important factor to determine the formation of irregular eutectic morphology.

It is interested to be noticed that regular eutectic morphologies shown as Fig. 8 can also be observed in the oxide eutectic, which is similar to that ever found in Al_2O_3/$GaAlO_3$ system.[25] This indicates that there exists the transition of irregular to regular growth manner caused by the large cooling rate during the rapid solidification of faceted phase.

3.3. Mechanical properties and toughening mechanism

The hardness and fracture toughness are determinated by Vickers indentation technique. The fracture toughness is calculated according to the equation proposed by Niihara for Palmqvist cracks if $l/a \leq 2.5$ or by Anstis for median cracks if $l/a \geq 2.5$, where l is crack length and a is half of indentation diagonal, which have been described elsewhere.[13,14] The mechanical

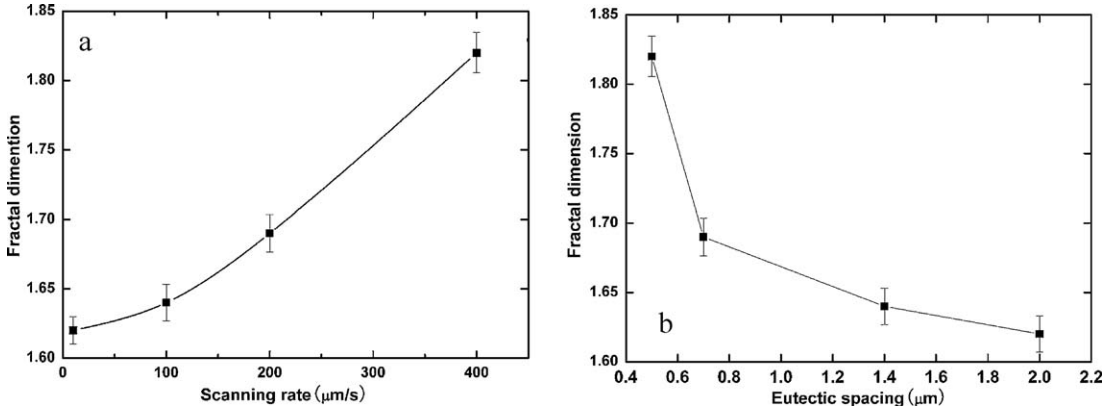

Fig. 6. Relationships of fractal dimension with laser scanning rate (a) and eutectic spacing (b) for the laser remelted Al_2O_3/YAG binary eutectic[22].

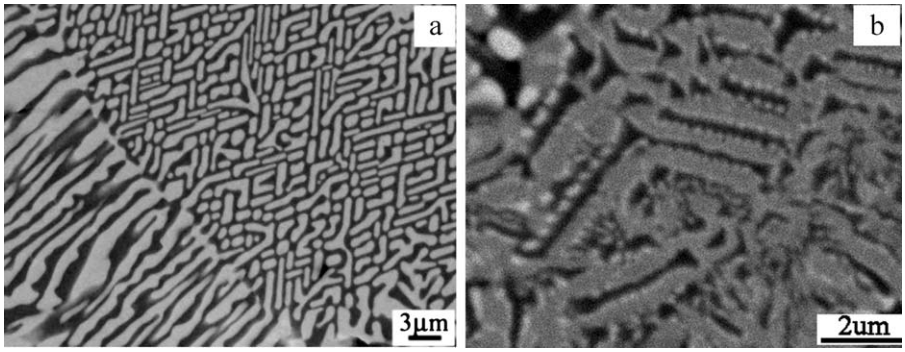

Fig. 8. The transition of irregular lamellae to regular rods (right) in transverse cross-section of the Al_2O_3/YAG binary eutectic grown by MEBFZM at 25 μm/s (a)[17] and the regular lamellae (alternate array of three phases) observed in the bottom region of the Al_2O_3/YAG/ZrO_2 ternary eutectic grown by LZM at the scanning rate of 80 μm/s (b).

properties of laser remelted Al_2O_3/YAG and Al_2O_3/YAG/ZrO_2 eutectics are listed in Table 2 in comparison with those reported in the literatures. It is shown that for Al_2O_3/YAG/ZrO_2, $H_V = 16.7 \pm 2.0$ GPa, $K_{IC} = 8.0 \pm 2.0$ MPa $m^{1/2}$; while for Al_2O_3/YAG, $H_V = 17.5 \pm 2.0$ GPa, $K_{IC} = 3.6 \pm 0.4$ MPa $m^{1/2}$. The fracture toughness of Al_2O_3/YAG/ZrO_2 ternary eutectic is obviously higher than that of Al_2O_3/YAG binary eutectic, which indicates that the addition of ZrO_2 phase and the microstructure refinement are helpful to increase the fracture toughness.

As compared with that of metallic alloy, the fracture toughness of DS oxide eutectic is very low, which severely restricts its practical application. It has always been the main point of research to reveal the toughening mechanism and to develop the toughening technique for oxide eutectic. Recently more efforts have been focused on how to enhance the resistance to crack propagation. So far, it is believed that the fracture toughness improvement for Al_2O_3-based eutectic *in situ* composite can be attributed to the following factors:

(1) *The crack arrest by interface*. As the microstructure refinement provides considerable amounts of heterophase interfaces, the crack propagation can be effectively retarded by the interfaces. As shown in Fig. 9a, a crack is stopped and another crack is initiated nearby, but both of them are eventually arrested by the interface.
(2) *The crack deflection and branching*. The crack deflection in Al_2O_3/YAG/ZrO_2 ternary eutectic is shown in Fig. 9b and c. The crack deflection at Al_2O_3/YAG interface is shown in Fig. 9b as the arrows indicated while the deflection at YAG/ZrO_2 interface is shown in Fig. 9c. Similar crack

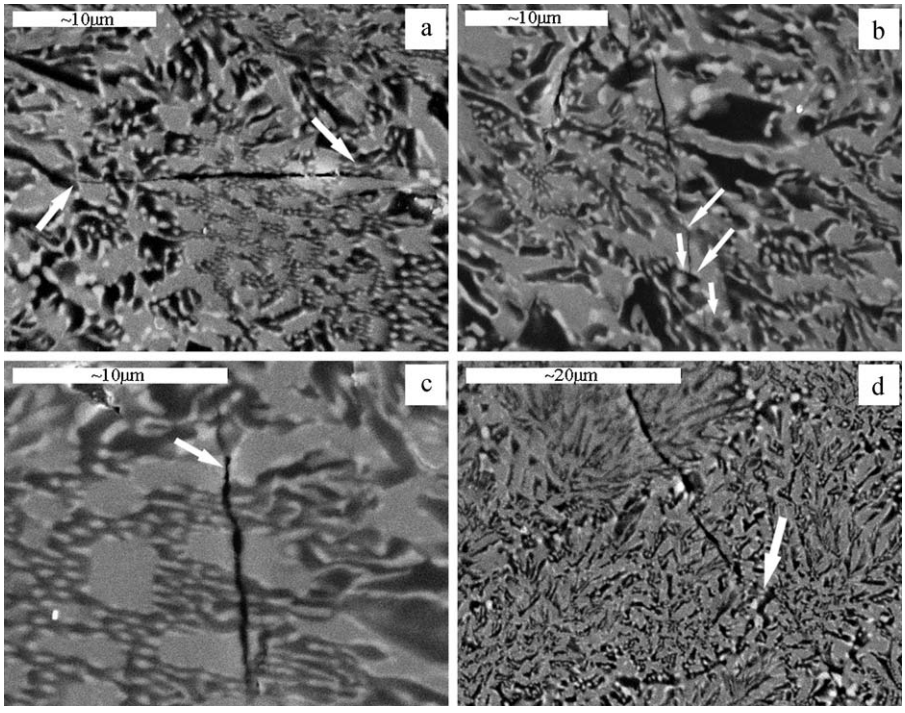

Fig. 9. The interaction of the crack path and the ternary eutectic microstructure in the Al_2O_3/YAG/ZrO_2 ternary eutectic grown at the scanning rate of 40 μm/s: (a) the cracks are arrested by the fine eutectic phases; (b) the cracks are deflected at the Al_2O_3/YAG interfaces; (c) the crack is deflected at the YAG/ZrO_2 interface; (d) the crack appears branching in the fine microstructure[13].

Table 2
Mean values of Vickers indentation hardness and fracture toughness for the directionally solidified Al_2O_3-based eutectic ceramic composite and correlative comparisons measured by the same method.

System	Vickers hardness (GPa)	Fracture toughness (MPa $m^{1/2}$)
Al_2O_3/YAG (our work)	17.5 ± 2.0	3.6 ± 0.4
Al_2O_3/YAG/ZrO_2 (our work)	16.7 ± 2.0	8.0 ± 2.0
Al_2O_3/YAG[26]	15–16	2–2.4
CeO_2-doped Al_2O_3/YAG[9]	34.7	4.99
ZrO_2 modified Al_2O_3–YAG[27]		5.6 ± 1.2
Al_2O_3/YAG/ZrO_2 [19]	14.8	4.3
Al_2O_3/YAG/ZrO_2 [28]		9.0 ± 2.0
Al_2O_3/YAG/ZrO_2 [29]	19.8	8.9
Al_2O_3/GAP/ZrO_2 [29]	17.9	8.5
Al_2O_3/YAG [30]		2–4 (SENB method)
Al_2O_3/YAG/YSZ [30]		5–5.3 (SENB method)

deflection is also found by Peña et al.[19] The crack deflection changes the crack propagation path and energy, resulting in the weakened crack to be easily arrested. As shown in Fig. 9d, the crack branching in Al_2O_3/YAG/ZrO_2 retards the crack growth and reduces the stress intensity of crack tip.

(3) *High thermal residual stress*. The thermal expansion coefficients of Al_2O_3 and YAG phases are all about $8.0 \times 10^{-6}\,K^{-1}$, but the value of ZrO_2 is $12.0 \times 10^{-6}\,K^{-1}$. The discrepancy in thermal expansion coefficients results in high thermal residual stress in Al_2O_3/YAG/ZrO_2. So Al_2O_3 and YAG are often subjected to compressive stress but ZrO_2 is subjected to tensile stress.[19] High residual tensile stress (>1 GPa) in ZrO_2 has been reported in Al_2O_3/YAG/ZrO_2 eutectics.[8] It is considered that the crack is preferred to be arrested in regions subjected to compressive stress since the crack propagation energy is extremely consumed and released.

4. Conclusions

The Al_2O_3/YAG binary eutectic and Al_2O_3/YAG/ZrO_2 ternary eutectic *in situ* composites are successfully fabricated by the laser zone melting technique, the modified electron beam floating zone melting technique and the laser direct forming technique under different growth conditions with high thermal gradients. The eutectics exhibit the solidification microstructure as "Chinese Script" pattern consisting of entangled network of eutectic phases. The eutectic spacing is extremely reduced due to rapid solidification and ZrO_2 addition. The minimum eutectic spacing is 100 nm. The Al_2O_3-based eutectic generally shows complex and irregular microstructure caused by faceted growth derived from high fusion entropy of eutectic phases. The transition of faceted to non-faceted growth morphology is also found. The hardness reaches 17.5 GPa and 16.7 GPa, and the fracture toughness reaches 3.6 MPa $m^{1/2}$ and 8.0 MPa $m^{1/2}$ for Al_2O_3/YAG and Al_2O_3/YAG/ZrO_2, respectively. The improved fracture toughness is mainly attributed to microstructure refinement and ZrO_2 addition, which leads to effective retardance of crack propagation by crack arrest, deflection, branching as well as high residual stress. The thorough research on solidification characteristic, eutectic growth manner and toughening mechanism of Al_2O_3-based eutectic are in progress in order to further develop the eutectic solidification theory and the preparation technique for high performance Al_2O_3-based eutectic ceramic *in situ* composite.

Acknowledgments

The authors would gratefully acknowledge the financial support from National Natural Science Foundation of China (50772090, 51002122), Provincial Natural Science Foundation of Shaanxi Province (2010JQ6005), Aeronautical Science Foundation of China (2010ZF53064), NPU Foundation for Fundamental Research (NPU-FFR-W01 8101, NPU-FFR-G9KY1016), Research Fund of the State Key Laboratory of Solidification Processing in NWPU (08-QZ-2008, 76-QP-2011), Opening Project of State Key Laboratory for Advanced Metals and Materials (2007AMM004) and the New People and New Directions Foundation of School of Materials Science and Engineering in NPU (09XE0104-5).

References

1. Ochiai S, Ueda T, Sato K, Hojo M, Waku Y, Nakagawa N, et al. Deformation and fracture behavior of an Al_2O_3/YAG composite from room temperature to 2023 K. *Compos Sci Technol* 2001;**61**:2117–28.
2. Hirano K. Application of eutectic composites to gas turbine system and fundamental fracture properties up to 1700 °C. *J Eur Ceram Soc* 2005;**25**:1191–9.
3. Mazerolles L, Perriere L, Lartigue-Korinek S, Piquet N, Parlier M. Microstructures, crystallography of interfaces, and creep behavior of melt-growth composites. *J Eur Ceram Soc* 2008;**28**:2301–8.
4. Llorca J, Orera VM. Directionally solidified eutectic ceramic oxides. *Prog Mater Sci* 2006;**51**:711–809.
5. Waku Y, Nakagawa N, Wakamoto T, Ohtsubo H, Shimizu K, Kohtoku Y. A ductile ceramic eutectic composite with high strength at 1873 K. *Nature* 1997;**389**:49–52.
6. Waku Y, Sakata S, Mitani A, Shimizu K. Temperature dependence of flexural strength and microstructure of Al_2O_3/YAG/ZrO_2 ternary melt growth composite. *J Mater Sci* 2002;**37**:2975–82.
7. Ramírez-Rico J, Pinto-Gómez AR, Martínez-Fernández J, de Arellano-López AR, Oliete PB, Peña JI, et al. High-temperature plastic behaviour of Al_2O_3–$Y_3Al_5O_{12}$ directionally solidified eutectics. *Acta Mater* 2006;**54**:3107–16.

8. Oliete PB, Peña JI, Larrea A, Orera VM, Llorca J, Pastor JY, et al. Ultra-high strength nanofibrillar Al_2O_3–YAG–YSZ eutectics. *Adv Mater* 2007;**19**:2313–8.
9. Kaiden H, Durbin SD, Yoshikawa A, Lee JH, Sugiyama K, Fukuda T. Model for the microstructure of oxide eutectics and comparison with experimental observations. *J Alloys Compd* 2002;**336**:259–64.
10. Park D-Y, Yang J-M. Fracture behavior of directionally solidified CeO_2- and Pr_2O_3-doped $Y_3Al_5O_{12}/Al_2O_3$ eutectic composites. *Mater Sci Eng A* 2002;**332**:276–84.
11. Lee JH, Yoshikawa A, Fukuda T. Growth of $MgAl_2O_4$/MgO eutectic crystals by the micro-pulling-down method and its characterization. *J Eur Ceram Soc* 2005;**25**:1351–4.
12. Larrea A, Orera VM, Merino RI, Peña JI. Microstructure and mechanical properties of Al_2O_3–YSZ and Al_2O_3–YAG directionally solidified eutectic plates. *J Eur Ceram Soc* 2005;**25**:1419–29.
13. Su HJ, Zhang J, Cui CJ, Liu L, Fu HZ. Rapid solidification of $Al_2O_3/Y_3Al_5O_{12}/ZrO_2$ eutectic *in situ* composites by laser zone remelting. *J Cryst Growth* 2007;**307**:448–56.
14. Su HJ, Zhang J, Cui CJ, Liu L, Fu HZ. Rapid solidification behaviour of $Al_2O_3/Y_3Al_5O_{12}$ (YAG) binary eutectic ceramic *in situ* composites. *Mater Sci Eng A* 2008;**479**:380–8.
15. Lakiza SM, Lopato LM. Stable and metastable phase relations in the system alumina–zirconia–yttria. *J Am Ceram Soc* 1997;**80**:893–902.
16. Caslavsky JL, Viechnicki DJ. Melting behavior of metastability of yttrium aluminum garnet (YAG) and $YAlO_3$ determined by optical difference thermal analysis. *J Mater Sci* 1980;**15**:1709–18.
17. Su HJ, Zhang J, Deng YF, Liu L, Fu HZ. A modified preparation technique and characterization of directionally solidified $Al_2O_3/Y_3Al_5O_{12}$ eutectic *in situ* composites. *Scripta Mater* 2009;**60**:362–5.
18. Lee JH, Yoshikawa A, Fukuda T, Waku Y. Growth and characterization of $Al_2O_3/Y_3Al_5O_{12}/ZrO_2$ ternary eutectic fibers. *J Cryst Growth* 2001;**231**:115–20.
19. Peña JI, Larsson M, Merino RI, de Francisco I, Orera VM, Llorca J, et al. Processing, microstructure and mechanical properties of directionally-solidified Al_2O_3–$Y_3Al_5O_{12}$–ZrO_2 ternary eutectics. *J Eur Ceram Soc* 2006;**26**:3113–23.
20. Cui CJ, Zhang J, Jia ZW, Su HJ, Liu L, Fu HZ. Microstructure and field emission properties of the Si-$TaSi_2$ eutectic *in situ* composites by electron beam floating zone melting technique. *J Cryst Growth* 2008;**310**:71–7.
21. Calderon-Moreno JM, Yoshimura M. Stabilization of zirconia lamellae in rapidly solidified alumina–zirconia eutectic composites. *J Eur Ceram Soc* 2005;**25**:1369–72.
22. Zhang J, Su HJ, Tang B, Liu L, Fu HZ. Fractal characteristic of laser zone remelted Al_2O_3/YAG eutectic *in situ* composite. *J Cryst Growth* 2008;**310**:490–4.
23. Harimkar SP, Dahotre NB. Characterization of microstructure in laser surface modified alumina ceramic. *Mater Charact* 2008;**59**:700–7.
24. Hunt JD, Jackson KA. Binary eutectic solidification. *AIEE* 1966;**236**:843–52.
25. Andreeta ERM, Andreeta MRBA, Hernandes C. Laser heated pedestal growth of $Al_2O_3/GdAlO_3$ eutectic fibers. *J Cryst Growth* 2002;**234**: 782–5.
26. Pastor JY, Llorca J, Salazar A, Oliete PB, de Francisco I, Peña JI, et al. Mechanical properties of melt-grown alumina–yttrium garnet eutectics up to 1900 K. *J Am Ceram Soc* 2005;**88**:1488–95.
27. Calderon-Moreno JM, Yoshimura M. Microstructure and mechanical properties of quasi-eutectic Al_2O_3–$Y_3Al_5O_{12}$–ZrO_2 ternary composites rapidly solidified from melt. *Mater Sci Eng A* 2004;**375–377**:1246–9.
28. Calderon-Moreno JM, Yoshimura M. Al_2O_3–$Y_3Al_5O_{12}$ (YAG)–ZrO_2 ternary composite rapidly solidified from the eutectic melt. *J Eur Ceram Soc* 2005;**25**:1365–8.
29. Mazerolles L, Piquet N, Trichet MF, Perrière L, Boivin D, Parlier M. New microstructures in ceramic materials from the melt for high temperature applications. *Aero Sci Tech* 2008;**12**:499–505.
30. Pastor JY, LLorca J, Martin A, Peña JI, Oliete PB. Fracture toughness and strength of Al_2O_3–$Y_3Al_5O_{12}$ and Al_2O_3–$Y_3Al_5O_{12}$–ZrO_2 directionally solidified eutectic oxides up to 1900 K. *J Eur Ceram Soc* 2005;**28**: 2345–51.